DOI 10.15826/urej.2018.2.2.002 УДК 537.871

Быстрое сегментирование среды вращающегося осесимметричного рассеивателя произвольной формы для численного анализа полей первого порядка

К. М. Зейде
Уральский федеральный университет имени первого Президента России Б. Н. Ельцина, Екатеринбург, Россия
k.m.zeyde@urfu.ru

Аннотация. В данной статье описывается алгоритм численного моделирования релятивистских эффектов распространения электромагнитных волн, возникающих в неинерциальных системах отсчета, а именно во вращающейся среде. Автор предлагает быстрый метод сегментирования геометрии диэлектрика, основанный на уточненных параметрах электромагнитной рефракции в среде (диэлектрическая и магнитная проницаемости), получаемых за счет пространственных гармоник в разложениях полей, с последующим выводом координатной зависимости постоянной распространения. Геометрия рассеивателя может быть произвольно осесимметричной, но с круговым поперечным сечением вдоль направления распространения электромагнитных волн. Точность моделирования оценивается в сравнении со строгими решениями, полученными ранее.

Ключевые слова. Постоянная распространения, релятивистские эффекты, численное моделирование, электромагнитная рефракция, сегментирование.

Fast Segmentation of a Rotating Axisymmetric Scatterer Medium of an Arbitrary Form for the First Order Fields Numerical Analysis

Kirill M. Zeyde
Ural Federal University, Ekaterinburg, Russia
k.m.zeyde@urfu.ru

Abstract. This paper describes an algorithm for numerical simulation of the propagation relativistic effects arising in noninertial reference systems and, in particular, in rotating media. The author proposes a fast segmentation method based on obtaining the electromagnetic refraction parameters of the medium (permittivity and permeability), due to spatial harmonics in the expansion of fields, and the subsequent derivation of the propagation constant in the coordinate dependence. The geometry of the scatterer may be arbitrary axisymmetric, but with a circular cross-section along the direction of prop-

agation. The accuracy of the modeling is estimated in comparison with analytics. The results of the simulation prove the effectiveness of the method.

Keyword. Propagation constant, relativistic effects, numerical simulation, electromagnetic refraction, segmentation.

Introduction

The expediency of studies of relativistic electrodynamics is defined by the fundamental possibility of detecting corresponding effects, due to highly sensitive equipment existing nowadays and new algorithms for big data processing. For practical purposes, such study is related to the problems of radio diagnostics (rotating parts of the machines), radio navigation (distortion of the signal due to rotating elements), geo-monitoring (the Earth is a rotating frame of reference in an external gravity field) and space exploration (rotating plasma columns, etc.). The theory of the propagation of electromagnetic waves in non-inertial reference frames is well developed [1–3], but the number of experiments is small, which is primarily associated with the weakness of the observable effects, which are indistinguishable in external factors (geomagnetic field, noise, vibration, etc.). The fast and accurate formulation of a numerical experiment on the scattering of the electromagnetic waves by a rotating object provides the necessary data for the subsequent use in a natural experiment. The implementation of this approach faces the lack of computational means for the description of the characteristics of the moving medium provided taking into account its morphology. The solution proposed in [4] describes the complete methodology of FDTD modeling. The time domain of the solution is not necessary — it may not be optimal in fast computations. The independent FEM solver introductory is noted in [5]. The conditions and possibilities for the technical application of targeted effects are detalized in the paper [6].

This paper shows an algorithm based on the segmentation of the scatterer geometry, where each segment is described by constant values of the dielectric and magnetic parameters. The combination of all segments determines the anisotropy of the medium. Segmented geometry may be analyzed in convenient commercial CAD using any suitable numerical methods and techniques.

The parameters of the scatterer medium are defined by transforming the propagation constant of the moving medium from the spatial harmonics to the coordinate dependence. In any case, this problem is solved by searching for the unknown function, which determines the spatial partition of the EM field. The axisymmetric object in the rotational dynamics around the symmetry axis retains its boundary conditions and allows solving the electrodynamic problem in the frequency domain, therefore the time factor is excluded from the field equations. For the same reason, any kind of the Doppler's effect is absent in the system under consideration. The classical solution is

based on the Maxwell — Minkowski equations [2]. In this paper, the constitutive equations are written only for the first order of the effect.

In fig. 1, *a* the plan view of the geometry of the system is shown. Section *XOY* is a circle, and this is a necessary condition for this method. In this context for $\rho \leqslant a$ any function of an independent coordinate φ describes the shape of the scatterer. The *Z* axis is the axis of symmetry of the scatterer, and also the axis of rotation. Parallel polarization (TM) corresponds to direction of vector E_i along *Z* axis (superscript "*i*" for incident field). The range of elevation angle θ in [0; π], describes the shape of the scatterer. In fig. 1, *b* the possible geometry of the scatterer on the side is shown. The silhouette function is the scatterer morphology function, describing the radius of the circle at each cross-section of the target (*a* and *a'*).

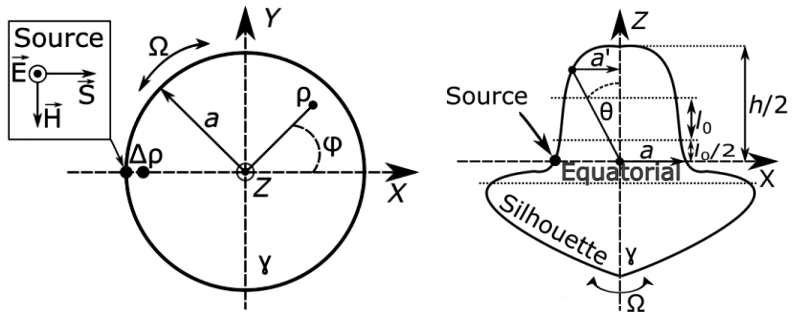

a *b*

Fig. 1. The system geometry (*a* — top view, *b* — side view)

Propagation

The analytical solution is invariant to the direction of rotation of the scatterer around the *Z* axis. It is enough to simply change the angular velocity sign (clockwise $\Omega < 0$, or counterclockwise $\Omega > 0$). In the obtained algorithm, the value of this quantity depends on the direction of propagation from the source, however, the sign remains unchanged. The direction of the electromagnetic drag by the rotating media may be determined from the value of the index of refraction along the radii of movement.

A. The two-dimensional problem

It has been pointed out that the source is located at the media boundary (as surface excitation) and the positive direction along the *X* axis should be described by the material propagation constant γ:

$$E_z^i = \frac{e^{-j\gamma x}}{e^{-j\gamma x_0}}, \qquad (1)$$

where subscript "0" for coordinates — the source position point. Expressing the propagation constant, it is obtained:

$$\gamma = \frac{j \ln\left[E_z^i \right]}{x - x_0}. \quad (2)$$

To formulate the two-dimensional problem, as the scatterer, the infinite circular cylinder along the Z axis is taken. To satisfy the propagation principle in the media, taking into account that the equation (2) meaningless for $|x| > a$ $x_0 = -a$ is taken. Performing the transition to the cylindrical coordinate system: $\rho_0 = a$ and $\varphi_0 = \pi$. The Fourier expansion of the cylindrical function for (1) is as follows:

$$E_z^i(n) = \frac{\sum_{n=-\infty}^{+\infty} j^{-n} J_n(\gamma_n \rho) e^{jn\varphi}}{e^{-jkx_0}}. \quad (3)$$

The expression (3) is the expansion of the field over spatial harmonics n, where k — the free space wavenumber. In the continuous field, each n is expressed as the function of coordinates (ρ; φ). The continuous propagation constant is now written as $\gamma = \frac{j \ln\left[E_z^i(n) \right]}{\rho \cos(\varphi) + a}$. (4)

The refraction parameters of the moving medium are different for different spatial harmonics of the field. In [3] and [7] γ_n was obtained in the form of the polynomial. The propagation constant is obtained in the strict form in the paper [8]. The solution of the wave equation involves the angle between the linear velocity of the media and the wave vector. Rigorous analysis of the arising spatial dispersion is problematic [9].

In this context, it is convenient to represent γ in the form corresponding to the perturbation theory. Grouping the summands of zero and the first order (subscripts "0" and "1") with the identification of the physical process that determines the disturbance of the medium, the following is acquired:

$$\gamma_n = \sqrt{k_0^2 + \Omega n k_1^2}, \quad (5)$$

where k_0 and k_1 the complex values of the wavenumbers:

$$k_0 = \sqrt{\frac{\omega^2 \mu_r \varepsilon_r}{c^2}}, k_1 = \sqrt{\frac{2\omega\left(N^2 - 1\right)}{c^2} + j\sigma\mu_0}. \quad (6)$$

To specify a stationary medium ε_r and μ_r may have an imaginary part, therefore $N = [\mathrm{Re}\,(\varepsilon_r)\mathrm{Re}\,(\mu_r)]^{0.5}$, σ is the conductivity of the medium and μ_0 is the magnetic constant.

The electrophysical interpretation of the characteristic kinematics of the target is expressed in terms of refined multiplication refraction index factors: $\varepsilon_{rr} = \varepsilon_r + \Delta_N$ and $\mu_{rr} = \mu_r + \Delta_N$, where

$$\Delta_N = -\frac{\omega(\varepsilon_r + \mu_r) - \sqrt{\mu_r{}^2\omega^2 - 2\mu_r\varepsilon_r\omega^2 + \varepsilon_r{}^2\omega^2 + 4\gamma^2c^2}}{2\omega}. \quad (7)$$

The mathematical part of the description of the algorithm is considered to be complete.

The set of input parameters 1 is taken for the cylinder: $f = 200$ MHz, $a = 0.955$ m, $\mu_r = 1 - 0j$, $\varepsilon_r = 4 - 0.2j$, $\Omega = 9.3 \cdot 10^6$ rad/s. Due to the indeterminacy of the field at the source, it is necessary to take into account the certain displacement (Δ_ρ) along the coordinate ρ inside the medium (fig. 1, *a*). For the well-conducting medium Δ_ρ can be related to the skin depth [10]. For the set of parameters 1 this proportion is not applicable due to the low conductivity of the medium ($\sigma = 0.00223$ S/m). In this context, the minimal spatial increment in the system is applied. At the source, functions (2) and (4) shows singularity. To avoid this situation, the slight perturbation in the coordinate ρ (functions are structurally nonstable) is introduced to determine the convergence of the limit ($\rho = \lim_{\Delta\rho \to 0} [a - \Delta_\rho a]$), which is determined by the iterative decrease of the displacement.

A possible modification of the problem is perpendicular polarization TE. As it's shown in [7], the function (3) retains its structure but rewrites it for the magnetic field.

B. The three-dimensional problem

Exactly the same source, in exactly the same position, in the presence of a sphere, as a scatterer, requires the introduction of two expansions, instead of one in (3). The resulting series corresponds to the mathematical apparatus of spherical harmonics [11] with two altering spatial harmonics *n* and *m*. In this case, equation (5) must describe the value of γ_{nm}.

Firstly, the velocity distribution relative to the position of the source (fig. 1, *b*) is determined. In connection to this, the angle θ describes the morphology of the scatterer even at arbitrary coordinates of the system. The linear velocity of each section of the sphere is equal to $\Omega\, a \sin(\theta)$.

Secondly, the cause of the perturbations is not a zero value Ω. The position function gets into the resulting expression for the propagation constant [11]. In (5), the position function includes $n\Omega$, as a perturbation parameter. The transition from the spatial harmonic to the coordinate dependence through the coefficient $\varkappa(\rho, \varphi)$:

$$\kappa(\rho, \varphi) = -\left(\frac{k_0}{k_1}\right)^2 - \left(\frac{\ln\left[E_z^i(n)\right]}{k_1\left(\rho\cos(\varphi) + a\right)}\right)^2. \quad (8)$$

Finally, for a sphere, the function of morphology sin (θ) also includes an expression for the propagation constant to satisfy the dependence of the second-type spatial harmonic:

$$\gamma = \sqrt{k_0^{\,2} + \kappa(\rho,\varphi)\sin(\theta)k_1^{\,2}}. \quad (9)$$

A generalization of the expression for any complex form of the targets yields:

$$\gamma = \sqrt{k_0^{\,2} + \kappa(\rho,\varphi)\frac{a'(\theta)}{a}k_1^{\,2}}. \quad (10)$$

For the sphere, the set of parameters 2 are defined as: $f = 50$ MHz, $a = 1$ m, $\mu_r = 1 - 0j$, $\varepsilon_r = 16 - 0.2$j, $\Omega = 1.5 \cdot 10^6$ rad/s.

Segmentation

Matrices ($\varepsilon_{C\theta xC\varphi}$) and ($\mu_{C\theta xC\varphi}$) describe the electro physical parameters of the segments, with the size $C\theta$ for the total number of allocated segments along the vertical section and $C\varphi$ in the horizontal section. A typical form of the permittivity matrix is given below:

$$\begin{pmatrix} \dot{\varepsilon}_{11} & \cdots & \dot{\varepsilon}_{1C\varphi} \\ \vdots & \ddots & \vdots \\ \dot{\varepsilon}_{C\theta 1} & \cdots & \dot{\varepsilon}_{C\theta C\varphi} \end{pmatrix}.$$

The fastest way to determine the value of Δ_ρ is to exclude the catastrophic behavior of the function Im [ε_{rr}] (φ), with the maximum value of Ω, in the vicinity of the source. Figs. 2 and 3 demonstrate the emergence of catastrophes when approaching the source. Figs. 2, *a*, 3, *a* show the monotonous behavior of the function, in contrast to fig. 2, *b*, 3, *b*: Δ_ρ takes the minimum possible value before the appearance of critical points.

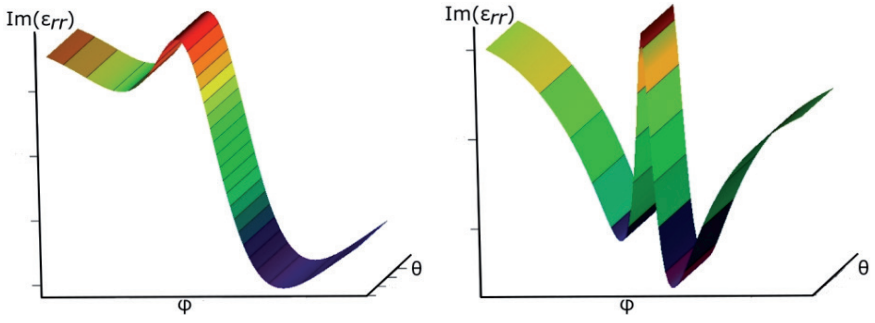

a *b*

Fig. 2. The structural instability of the function in the vicinity of $\varphi = 180°$ for the set of parameters 1; *a* for $\Delta_\rho = 10^{-3}$, *b* for $\Delta_\rho = 10^{-4}$

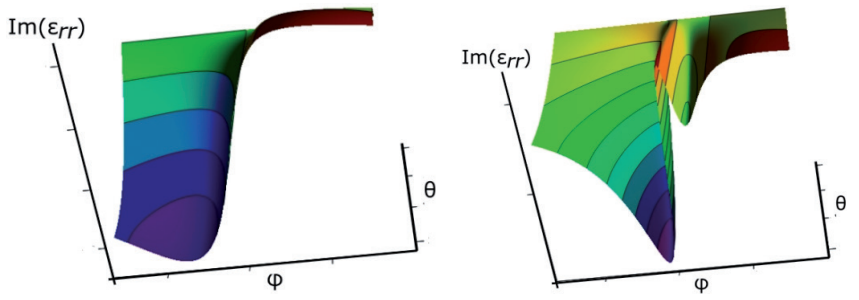

a *b*

Fig. 3. The structural instability of the function in the vicinity of φ = 180° for the set of parameters 2; *a* for $\Delta_\rho = 10^{-3}$, *b* for $\Delta_\rho = 10^{-4}$

The angular sector of segmentation — α, corresponds to the part of the topology, where Re $[\varepsilon_{rr}] \neq$ Re $[\varepsilon_r]$ defines the range for φ, which usually writes as $[\alpha_0; \alpha_1]$ (fig. 4). The value l_0 is an optimization parameter and in the fast method is chosen proceeding from the basic principles of the elementary scatterers.

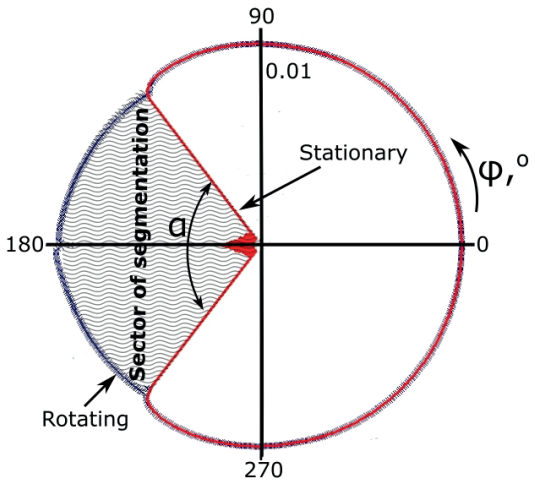

Fig. 4. Definition of the decomposition sector

The value *C*θ depends on the increment of the elevation angle, which is set manually and also affects the accuracy. This formulation is strongly related to the morphology of the scatterer. If the radius changes smoothly, the increment of the elevation angle is large. A sharp change in the geometry forming the silhouette should be described accurately.

The score for *C*φ is satisfied at θ = π/2, which corresponds to the equatorial plane of the scatterer (fig. 1, *b*, where *h* — the height of the scatterer). The number of horizontal segments depends on the expected accuracy of the

calculations. The optimal choice is based on a statistical sample of the actual parameters of the segment: at angles where the function is smooth and monotonic, it is logical to choose the average value of the parameter. Extremums or singular points of the function are described by a single small segment with the exact value of the absolute maximum.

The resulting matrix describes the electro physical parameters of the medium in the following direction: the element (11) corresponds to the segment $\varphi = \alpha_0$ and $\theta = 0$, the element ($C\theta C\varphi$) to the segment $\varphi = \alpha_1$ and $\theta = -\pi/2$. Because of propagation along the normal, not of interest, the edge of the segment is located in [8].

A. Infinite circular cylinder

One of the possible segmentation for the set of parameters 1 is as follows: $\Delta_\rho = 0.005$, $\alpha = [122; 231]^\circ$. The matrix of the medium is obtained as: $\alpha = 122-177^\circ$ is the average value of the parameters, $\alpha = 177-180^\circ$ and $\alpha = 180-183^\circ$ are the extrema of the quantity, $\alpha = 183-231^\circ$ is the mean value. The resulting matrices are given below:

$$\varepsilon_{1\times4} = \begin{pmatrix} 3.65- & 3.99- & 6.53- & 4.45- \\ 0.18j & 0.18j & 0.18j & 0.27j \end{pmatrix},$$

$$\mu_{1\times4} = \begin{pmatrix} 0.65- & 0.99- & 3.53- & 1.45- \\ 0.02j & 0.09j & 0.21j & 0.04j \end{pmatrix}.$$

The geometry is presented at the fig. 5, *a*.

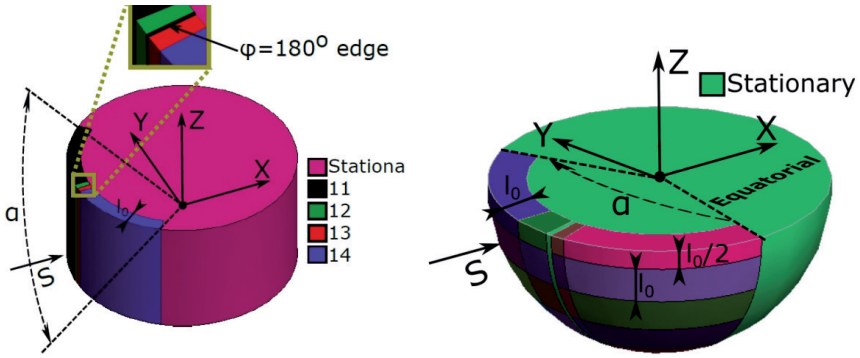

a *b*

Fig. 5. Fast segmentation (*a* — infinite circular cylinder, *b* — sphere)

B. Sphere

Trivial geometry in the case of segmentation of the sphere gives the formulation for the elevation angle: $\theta = \pi/2 - a\sin(c_\theta l_0/a)$. The silhouette function $a'(\theta)$ is smooth and without singular points, that is why, according to fig. 1, *b*, the elevation angle is formed between the radius of the sphere

drawn to the middle of the segment c_θ, and the radius of the cross-section drawn at the same point.

To confirm the simulation, this paper proposes the following segmentation map for the 2 parameters set: $\Delta_\rho = 0.0005$, $\alpha = [105; 255]^\circ$. The medium matrix is defined as: $\alpha = 105–164^\circ$ is the mean value, $\alpha = 165–178^\circ$ is the extremum of the quantity, $\alpha = 180^\circ$ is the actual value, $\alpha = 181–185^\circ$ is the extremum and $\alpha = 186–255^\circ$ is the mean value. Note that $c_\theta = 5$, corresponds to the equatorial region. Because of the symmetry of the scatterer along the X axis, the parameter matrices are mirrored with respect to the row of the equatorial region. Below is the upper part of the matrix of permittivity and in fig. 5, *b* the lower part of the sphere. Each element of the permeability matrix has the same imaginary part as the corresponding permittivity matrix element, and for the real part, the expression: $\varepsilon_{rr} — \varepsilon_r = \mu_{rr} — \mu_r$, is valid.

$$\varepsilon_{9\times5} = \begin{pmatrix} 16.04+ & 16.41+ & 16 & 15.76- & 15.98- \\ 0.012j & 0.12j & & 0.03j & 0.007j \\ 16.1+ & 16.94+ & 16 & 15.42- & 15.94- \\ 0.03j & 0.26j & & 0.08j & 0.016j \\ 16.12+ & 17.17+ & 16 & 15.26- & 15.93- \\ 0.035j & 0.323j & & 0.1j & 0.02j \\ 16.13+ & 17.3+ & 16 & 15.18- & 15.92- \\ 0.04j & 0.356j & & 0.12j & 0.022j \\ 16.13+ & 17.32+ & 16 & 15.16- & 15.92- \\ 0.04j & 0.359j & & 0.123j & 0.023j \\ \dots & \dots & \dots & \dots & \dots \end{pmatrix}.$$

Results

Validation of analytical and model results produces according to the IEEE standard 1597.1–2008 [12]. The FSV procedure is initialized for every two sets of data to obtain the total value of the GDM [13]. To estimate the absolute average magnitude of the discrepancy, a differential point-to-point comparison (<Di> is the median of the differential point function) is performed. In the semi-analytic approach, the function (3) is sought for n [–60; 60]. Modeling and simulation are performed in the CAD of electromagnetic analysis Altair FEKO.

Justification of the proposed algorithm may be given only when compared with rigorous solutions. For an infinite circular cylinder, the necessary information is given in [3] and [7]. In particular, the set of parameters 1 exactly corresponds to the examples given in [7]. In this case, MoM/MLFMM is used. The average size of the mesh triangular element is approximately equal to l_0, periodic boundaries along the Z axis are taken into account. The resulting graphs are shown in figs. 6 and 7.

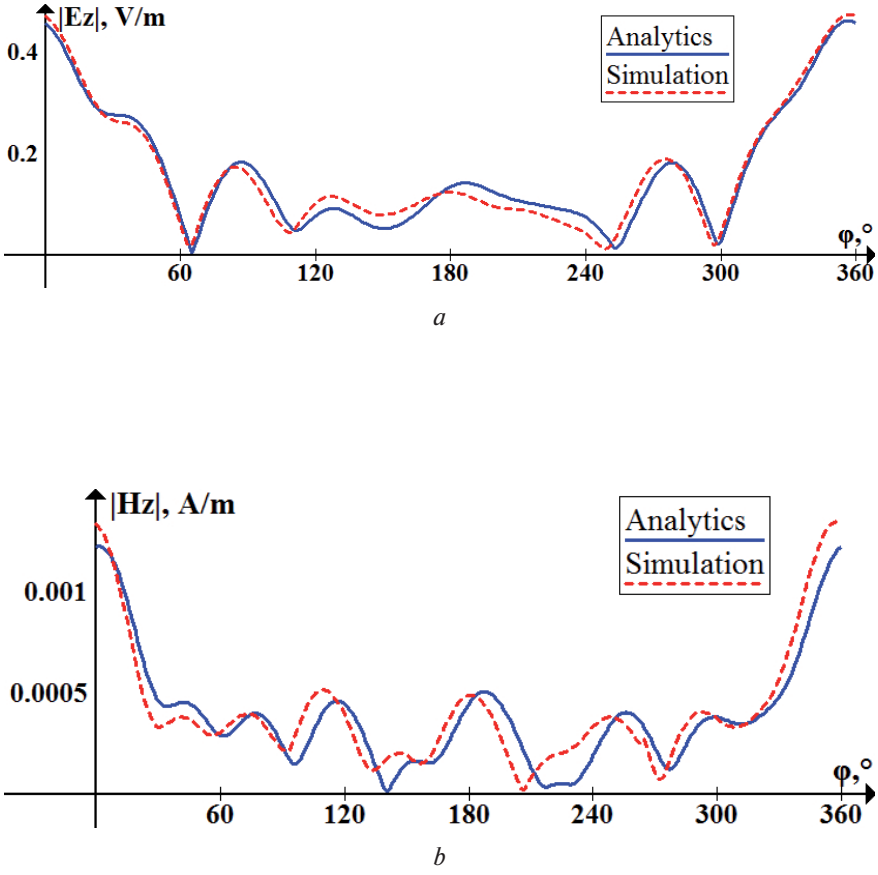

Fig. 6. Analytical and simulation results for the field distribution along the circle in *XOY* plane with radius 10 m for set of parameters 1: *a* — parallel polarization (GDM total = 0.2695, $< D_i > = 0.0182$ V/m); *b* — perpendicular polarization (GDM total = 0.557, $< D_i > = 0.0001$ A/m)

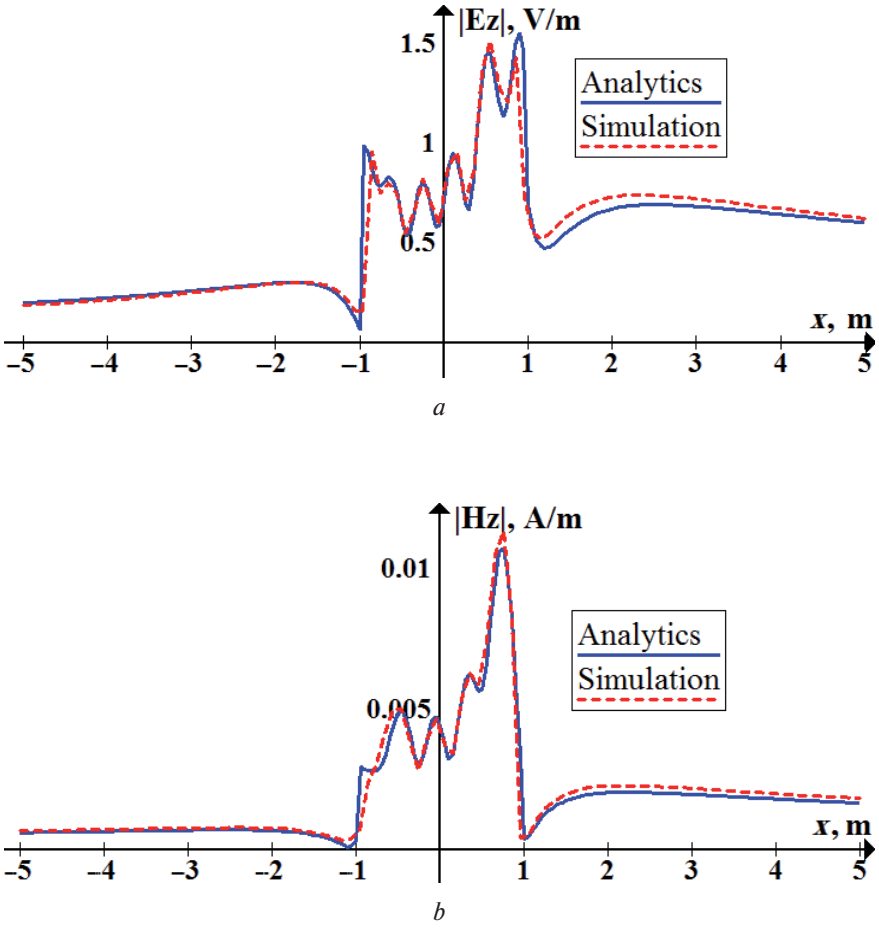

Fig. 7. Analytical and simulation results for the field distribution along the X axis for set of parameters 1: *a* — parallel polarization (GDM total for $x > 0 = 0.3572$, $< D_i >$ for $x > 0 = 0.0512$ V/m, GDM total for $x < 0 = 0.3527$, $< D_i >$ for $x < 0 = 0.024$ V/m); *b* — perpendicular polarization (GDM total for $x > 0 = 0.2347$, $< D_i >$ for $x > 0 = 0.0003$ A/m, GDM total for $x < 0 = 0.2994$, $< D_i >$ for $x < 0 = 0.0001$ A/m)

In the three-dimensional case, only the sphere provides the necessary analytics. Sources for comparing the results: [5] and [11]. In CAD for this geometry, FEM is used with the mean value of the length of the finite element equal to 0.098 m ($\approx l_0/2.35$). The resulting graphs are shown in fig. 8.

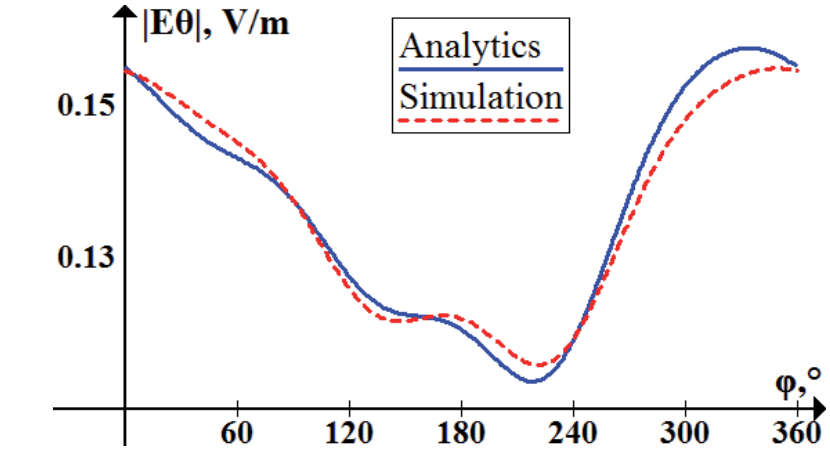

a

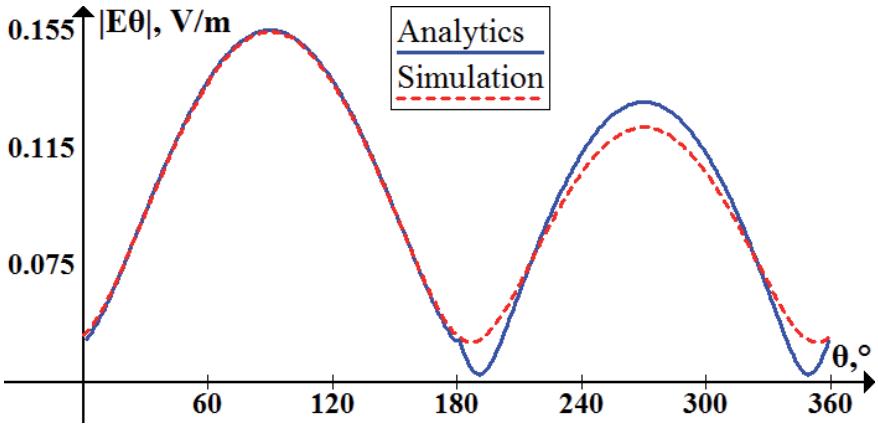

b

Fig. 8. Analytical and simulation results for the field component distribution along the circle with radius 10 m for set of parameters 2 and parallel polarization:

a — *XOY* plane (GDM total = 0.6144, $< D_i > = 0.002$ V/m);

b — *XOZ* plane (GDM total = 1.1592, $< D_i > = 0.0036$ V/m)

Analyzing the results obtained, the fact that the fast method of segmentation, which does not take into account the a priori modeling error is stated, the accuracy obtained is acceptable.

Conclusion

The presented comparison of computational and analytical results gives an idea of the lowest threshold for accuracy since it is based on fast segmentation, which does not use any optimization or variational algorithms. The used segmentation methodology is applied to the primary principles of decomposition, since the development of these principles is a separate scientific task.

The obtained results can serve as a confirmation of the effectiveness of the proposed method. The development of the principles of optimal segmentation is a crucial factor in this problem.

In conclusion, the main advantages and disadvantages of the segmentation approach should be pointed out. Among the disadvantages are the following:

- The presence of uncertainties in the method, which complicates the optimal choice. Ambiguities in the direction of distribution, choice α and especially Δ_ρ, explain this position.
- Manual generation of segmentation maps for each individual scatterer and system as a whole. In addition to the drawbacks described above, the matrices of the electrophysical parameters of the segments may contradict the principles of the automated engineering.
- The doubtful possibility of modeling toroidal geometries and other shapes with non-circular cross-section along the X axis.

The main advantages of the method are:

- The effective use of the functionality of the selected electromagnetic simulation software and its interface.
- Ample opportunities in time-accurate optimization of the model (semi-analytical adaptation, segmentation map, mesh creation rules, the simulation method).

The general problem of segmentation accuracy is explained by the adoption of different formulation to a certain degree of decomposition algorithms, for example, as in [14] and [15].

References

1. Van Bladel J. *Electromagnetic fields*. IEEE Press, 2007. Pp. 943–1000.

2. Shiozawa T. Phenomenological and electron-theoretical study of the electrodynamics of rotating systems. *Proc. of the IEEE*, 1973, vol. 61, no. 12.

3. Van Bladel J. Electromagnetic fields in the presence of rotating bodies. *Proc. of the IEEE*, 1976, vol. 64, no. 3.

4. Sahrani S., Iwamatsu H., Kuroda M. A novel approach for the analysis of electromagnetic field with rotating body. *ACES Journal*, 2011, vol. 26, no. 8, pp. 651–659.

5. Brignone M., Ramakrishnan P. K., Raffetto M. A first numerical assessment of the reliability of finite element simulators for time-harmonic electromagnetic problems involving rotating axisymmetric objects. *Proc. EMTS*, Espoo, 2016.

6. Van Bladel J. Relativity and engineering. *Springer Series in Electrophysics*, 1984, vol. 15, Berlin.

7. De Zutter D. Scattering by a rotating circular cylinder with finite conductivity. *IEEE Trans. Antennas Propagat.*, 1983, vol. AP-31, no.1, pp. 166–169.

8. Collier J. R., Tai C. T. Propagation of plane waves in lossy moving media. *IEEE Trans. Antennas Propagat.*, 1964, vol. 12, no.3, pp. 375–376.

9. Ryzhov Yu. A., Tamoikin V. V., Tatarskii V. I. Spatial dispersion of inhomogeneous media. *JETP*, 1965, vol. 21, no.2, pp. 433–438.

10. Zeyde K. M. Linear dependences of secondary field parameters versus angular velocity of scatterer. *Proc. SibCON*. Omsk, 2015.

11. De Zutter D. Scattering by a rotating dielectric sphere. *IEEE Trans. Antennas Propagat.*, 1980, vol. AP-28, no.5, pp. 643–651.

12. IEEE standard for validation of computational electromagnetics computer modeling and simulations, IEEE Std 1597.1, 2008.

13. Duffy A., Orlandi A. A review of statistical methods for comparing two data sets. *ACES Journal*, 2008, vol. 23, no. 1, pp. 90–97.

14. Kyurkchan A. G., Smirnova N. I. The solution of diffraction problems by a method of elementary scatterers. *EW and ES*, 2011, vol.16, no.8.

15. Schaubert D. H., Wilton D. R., Glisson A. W. A tetrahedral modeling method for electromagnetic scattering by arbitrarily shaped inhomogeneous dielectric bodies. *IEEE Trans. on Antennas and Propagat.,* 1984, vol. AP-30, no.1.

Информация об авторе

Зейде Кирилл Михайлович — ведущий инженер, старший преподаватель, ФГАОУ ВО «Уральский Федеральный Университет им. первого Президента России Б. Н. Ельцина», Екатеринбург, Россия

Information about the author

Zeyde Kirill Mikhailovich — leading engineer, senior lecturer, Ural Federal University, Ekaterinburg, Russia

Поступила / Receiver: 15.05.2018
Принята в печать / Accepted: 14.07.2018